



Cite this: *React. Chem. Eng.*, 2025, 10, 1216

Received 14th March 2025,
 Accepted 22nd April 2025

DOI: 10.1039/d5re00119f

rsc.li/reaction-engineering

Photocatalytic evolution of nitrous oxide from nitric monoxide over Pt-loaded titanium dioxide under UV irradiation†

Ryo Asayama,^{‡a} Masanori Takemoto,^{id ‡a} Arata Suzuki,^a Ryuichi Watanabe,^a Fuminao Kishimoto,^{id a} Kenta Iyoki,^{id abc} Tatsuya Okubo,^{id a} and Toru Wakihara,^{id *ad}

This study presents a photocatalytic evolution of nitrous oxide (N₂O) from nitric monoxide (NO), well known as a harmful gas contained in exhaust gas. Pt nanoparticles (NPs) were loaded on titanium dioxide (TiO₂) using different methods including impregnation, photo-deposition and chemical reduction methods. Bare TiO₂ (without metal loading) did not exhibit high N₂O evolution under UV irradiation, but all Pt-loaded TiO₂ photocatalysts did exhibit improved N₂O evolution.

Despite nitrous oxide (N₂O) being the “third” greenhouse gas, it has recently attracted attention in various fields. In the petrochemical industry, selective oxidation of hydrocarbons is vital for producing valuable fine chemicals,¹ and there has been growing interest in utilizing green and atom-efficient oxidants such as H₂O₂ and N₂O for catalytic oxidation.² Both H₂O₂ and N₂O release monoatomic oxygen, forming harmless H₂O and N₂, respectively. N₂O, in particular, is suitable as an oxidant in liquid and gas-phase reactions due to its high solubility in nonpolar media and gaseous nature. For instance, catalytic oxidation of CH₄ into methanol using N₂O over zeolites has been proposed, converting two greenhouse gases into a useful chemical.^{3,4} In the medical field, the demand of N₂O, also known as “laughing gas,” has been increasing.^{5,6} Considering these advantages, N₂O holds significant potential for clean technologies in fine chemical synthesis and medical developments.

Plant-scale manufacturing of N₂O was done at Jinhong Gas and Heng'an Gas Co., Ltd., where the decomposition of NH₄-

NO₃ is used for N₂O production. According to interviews with these companies, N₂O produced through the current process is available to only high-end users in practical applications because of the high cost of the process (approximately 3000–5000 \$ per Mg).⁷ The oxidation of NH₃ is considered an alternative reaction for N₂O production.^{7,8} However, there are concerns about the current price increase of NH₃, which is probably a barrier to achieving inexpensive N₂O production. As is well known, anthropogenic N₂O is mainly released into the atmosphere during agricultural and industrial activities,⁹ and N₂O capture can be a promising technique for the effective utilization of N₂O.^{10,11} However, the concentration of N₂O in the atmosphere is quite low (approximately 0.3–0.4 ppm). Many types of gas molecules, such as CO₂ and H₂O, are also present in the atmosphere, which makes selective separation of N₂O in the atmosphere further challenging. Considering the future demand of N₂O, further implementation of low-cost N₂O production is highly recommended.

Nitric monoxide (NO) is a well-known gaseous pollutant that mainly comes from the exhaust gases of automobiles, plants, and thermal power stations. In current de-NO_x systems, NO is converted into N₂ through selective catalytic reduction with NH₃ over zeolites^{12,13} or V-based TiO₂.^{14,15} before being discharged into the atmosphere. Recently, the use of NO as a feed gas for valuable nitrogen compounds has been a focus of research. For example, in several studies, the catalytic conversion of NO to NH₃ has been investigated.^{16–20} Thus, NO has great potential as a feed gas toward the low-cost production of N₂O.

Here, the photocatalytic evolution of N₂O from NO as the feed gas over Pt-loaded TiO₂ is reported. Pt NPs were loaded onto TiO₂ (P25) using different loading methods. The photocatalysts hardly converted NO into N₂O without ultraviolet (UV) irradiation, and the amount of N₂O evolved increased under UV irradiation. Additionally, the Pt-loaded TiO₂ photocatalyst exhibited higher N₂O evolution than did the bare TiO₂ photocatalyst, suggesting that Pt species can act as active sites in this case. These findings should help

^a Department of Chemical System Engineering, The University of Tokyo, 7-3-1 Hongo, Bunkyo-ku, Tokyo 113-8656, Japan. E-mail: wakihara@chemsys.t.u-tokyo.ac.jp

^b Precursory Research for Embryonic Science and Technology (PRESTO), Japan Science and Technology Agency (JST), Kawaguchi, Saitama 332-0012, Japan

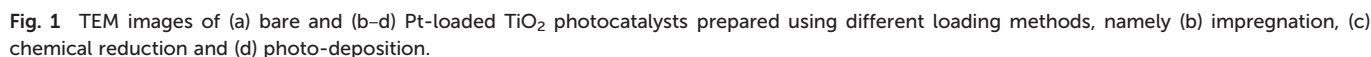
^c Department of Environment Systems, The University of Tokyo, 5-1-5 Kashiwanoha, Kashiwa-shi, Chiba 277-8563, Japan

^d Institute of Engineering Innovation, The University of Tokyo, 2-11-16 Yayoi, Bunkyo-ku, Tokyo 113-8656, Japan

† Electronic supplementary information (ESI) available. See DOI: <https://doi.org/10.1039/d5re00119f>

‡ These authors contributed equally.





Pt-loaded TiO_2 photocatalysts were synthesized using different loading methods, including chemical reduction, impregnation, and photo-deposition methods, and are denoted as Pt/ TiO_2 -cr, Pt/ TiO_2 -imp and Pt/ TiO_2 -pd, respectively. The details of the syntheses and characterizations of the photocatalysts are described in the ESI.† Fig. 1 shows transmission electron microscopy (TEM) images of the bare and Pt-loaded TiO_2 photocatalysts. Bare P25 was composed of small TiO_2 NPs with diameters of less than 20 nm, as shown in Fig. 1(a). Spherical Pt NPs were located on the surface of the TiO_2 NPs, and the Pt particles were less than 10 nm in diameter, as shown in Fig. 1(b–d). X-ray diffraction confirmed that the crystalline phase and the crystalline sizes of TiO_2 were not affected by Pt loading (Fig. S1, Table S1†). All of the Pt-loaded TiO_2 samples became black in color upon being loaded with Pt,

and UV-vis spectra of the Pt-loaded TiO_2 indicated light absorption in the visible-light region, due to the surface plasmon resonance of Pt NPs (Fig. S2†). The characteristics of the Pt NPs in the Pt-loaded TiO_2 photocatalysts are summarized in Table S1.† TEM images indicated that the particle sizes of Pt followed in the order $\text{Pt/TiO}_2\text{-cr} > \text{Pt/TiO}_2\text{-pd} > \text{Pt/TiO}_2\text{-imp}$. Dispersion of Pt determined from CO pulse measurements followed in the order $\text{Pt/TiO}_2\text{-imp} > \text{Pt/TiO}_2\text{-pd} > \text{Pt/TiO}_2\text{-cr}$. These results confirmed that the accessible surface area of the Pt NPs followed in the order $\text{Pt/TiO}_2\text{-imp} > \text{Pt/TiO}_2\text{-pd} > \text{Pt/TiO}_2\text{-cr}$. X-ray fluorescence revealed that there was no significant difference in Pt content among the three photocatalysts (1.7–1.8 wt%). Therefore, the three Pt-loaded TiO_2 photocatalysts with almost the same amount of Pt NPs and with different particle sizes were obtained.

Photocatalytic conversions of NO into N₂O over Pt-loaded TiO₂ photocatalysts were investigated using a quartz fixed-



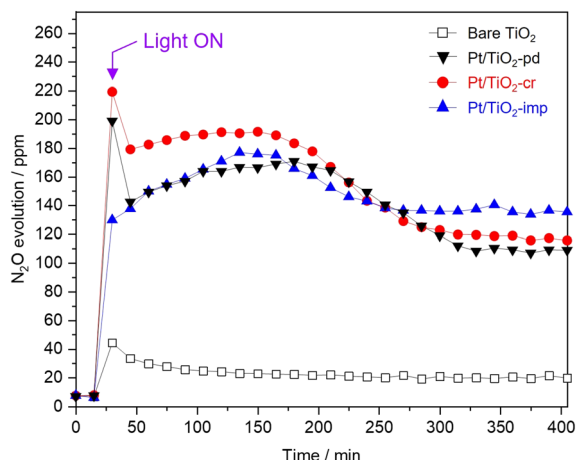


Fig. 3 N_2O evolutions over different photocatalysts. Photocatalytic tests were carried out at an SV of 3500 h^{-1} .

bed reactor made in house (Fig. 2). Typically, the input gas was passed through the water tank, and UV light was irradiated onto the upper side of the photocatalysts. Prior to photocatalytic tests, samples were pre-treated to completely rid them of carbon species. The details for the photocatalytic tests are described in ESI.† N_2O evolutions over different photocatalysts were compared in Fig. 3. None of the photocatalysts without UV irradiation produced any considerable amount of N_2O . Upon UV irradiation, the evolved amount of N_2O over bare TiO_2 increased to some extent, and considerably more so did ($>100 \text{ ppm}$) over each of the three Pt-loaded TiO_2 photocatalysts. These results were indicative of N_2O evolution having been accelerated by light irradiation and of Pt NPs playing a key role in enhancing N_2O evolution. Reaction mechanism is hereafter discussed using Pt/ TiO_2 -pd as the photocatalyst.

Fig. 4 shows representative gas chromatography (GC) profiles of the outlet gases in the photocatalytic tests under UV irradiation. No considerable peak was observed under He flow (in the absence of NO). When NO/He was introduced as

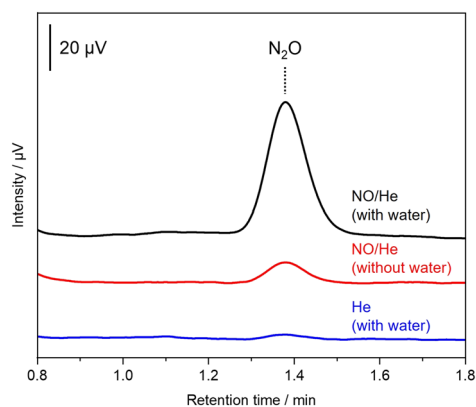


Fig. 4 GC profiles of the gases produced from different feed stocks. The catalytic tests were carried out using Pt/ TiO_2 -pd under UV irradiation at an SV of 3500 h^{-1} .

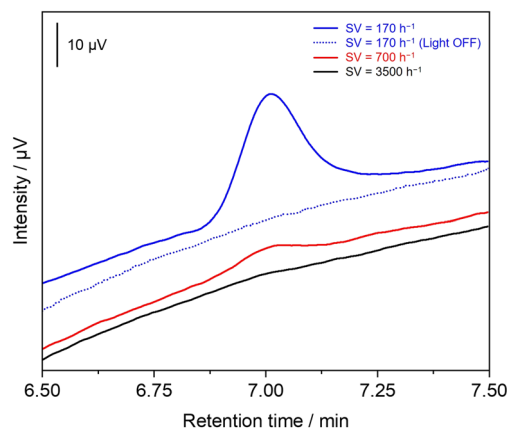


Fig. 5 GC profiles of the product gas over Pt/ TiO_2 -pd under UV irradiation at different SV conditions.

the feedstock gas, there was a peak at 1.36 min, which could be assigned to N_2O . This result indicated that N_2O evolved from the introduced NO. A decreased N_2O evolution was observed when water was not introduced into the reaction system, suggestive of water also playing a part in the photocatalytic reaction.

Fig. 5 shows GC profiles in the region of 6.5–7.5 min at various gas hourly space velocity (GHSV) values. No peak was observed at 7 min for a GHSV of 3500 h^{-1} (black line), but peaks at 7 min became obvious at lower GHSV values (red and blue lines). These peaks can be assigned to O_2 . Furthermore, the peaks originating from O_2 evolution were not observed at 7 min without UV irradiation (dashed, blue line). In summary, O_2 evolution was found to be triggered by UV irradiation together with N_2O evolution from NO feed stock. Fig. 6 shows a schematic illustration explaining the proposed mechanism for photocatalytic evolution of N_2O over TiO_2 with Pt loading. The reductive/oxidative and overall reactions of this system were estimated, and each potential *versus* a normal hydrogen electrode (NHE) can be presented as follows.

Reductive reaction:

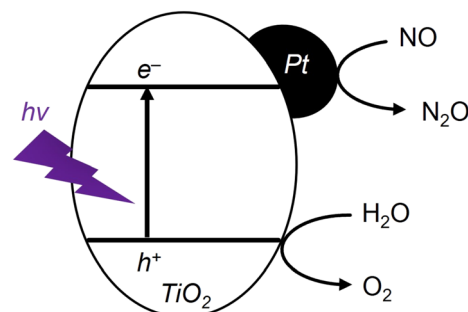
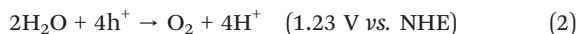


Fig. 6 Proposed mechanism for N_2O evolution over Pt-loaded TiO_2 under UV irradiation.



Oxidative reaction:



Overall reaction:



Considering the band positions of TiO_2 (conduction band: -0.38 V vs. NHE , valence band: 2.82 V vs. NHE),^{21,22} this photocatalytic reaction (eqn (1) and (2)) would be expected to be able to proceed. Furthermore, consideration of the calculated equilibrium conversion rate (Fig. S3†) suggested the overall reaction (eqn (3)) to be thermodynamically accessible. As for O_2 in this reaction, inspection of the stoichiometry of eqn (3) would suggest an evolution of half as much O_2 as N_2O by molarity, but the measured amount of evolved O_2 was considerably lower (Fig. S4†). Nitrogen dioxide (NO_2) was detected in the outlet gas by using a Fourier transform infrared detector, suggesting that some of the O_2 reacted with unreacted NO to form (NO_2) as shown in eqn (4).



As shown in Fig. 3, Pt loading was observed to enhance the photocatalytic evolution of N_2O , attributed to efficient separation of photogenerated charges. The apparent quantum yield (AQY) was calculated to be 4.4%. This value was comparably higher in gas-phase photocatalysis. Previous research showed the hygroscopic nature of the metal oxide having dramatically increased the AQY of photocatalytic water splitting.^{23,24} In the currently investigated N_2O evolution reaction, Pt-loaded TiO_2 seemed to be quite hygroscopic, resulting in high AQY.

In summary, low-cost N_2O manufacturing approach using NO as feed was proposed. The photocatalysts tested hardly converted NO into N_2O without UV irradiation, and the amount of N_2O that evolved increased under UV irradiation. In particular, the Pt-loaded TiO_2 photocatalyst exhibited higher N_2O evolution than did the bare TiO_2 photocatalyst, suggesting that Pt enhanced the efficiency of photogenerated charges. Furthermore, decreased evolution of N_2O was observed without H_2O , indicative of the involvement of H_2O in this photocatalytic reaction. To the best of our knowledge, this was the first study to demonstrate the photocatalytic evolution of N_2O from NO . Although further improvements (e.g., suppression of oxidation of NO and increase of conversion rate) is still required, these findings should be considered to help promote the development of N_2O production from a low-cost feedstock.

Data availability

The data that support the findings of this study are openly available.

Conflicts of interest

There are no conflicts to declare.

Acknowledgements

This work was partly supported by the New Energy and Industrial Technology Development Organization (NEDO) under the Moonshot Project, the Japan Society for the Promotion of Science (JSPS), a KAKENHI Grant-in-Aid for Transformative Research Areas (A) JP20A206/20H05880, a Grant-in-Aid for Scientific Research (S) JP23H05454, a Grant-in-Aid for Early-Career Scientists JP24K17585 and the Materials Processing Science project ("Materealize") of MEXT, Grant Number JPMXP0219192801.

References

- 1 V. N. Parmon, G. I. Panov, A. Uriarte and A. S. Noskov, *Catal. Today*, 2005, **100**, 115–131.
- 2 K. Severin, *Chem. Soc. Rev.*, 2015, **44**, 6375–6386.
- 3 P. Xiao, Y. Wang, Y. Lu, T. De Baerdemaeker, A.-N. Parvulescu, U. Müller, D. De Vos, X. Meng, F.-S. Xiao, W. Zhang, B. Marler, U. Kolb, H. Gies and T. Yokoi, *Appl. Catal., B*, 2023, **325**, 122395.
- 4 P. Xiao, Y. Wang, K. Nakamura, Y. Lu, T. De Baerdemaeker, A.-N. Parvulescu, U. Müller, D. De Vos, X. Meng, F.-S. Xiao, W. Zhang, B. Marler, U. Kolb, R. Osuga, M. Nishibori, H. Gies and T. Yokoi, *ACS Catal.*, 2023, **13**, 11057–11068.
- 5 A. C. Huizink, *Curr. Opin. Psychol.*, 2022, **45**, 101312.
- 6 M. A. Gillman, *Curr. Drug Res. Rev.*, 2019, **11**, 12–20.
- 7 Z. Tang, I. Surin, A. Rasmussen, F. Krumeich, E. V. Kondratenko, V. A. Kondratenko and J. Perez-Ramirez, *Angew. Chem., Int. Ed.*, 2022, **61**, e202200772.
- 8 D. R. MacFarlane, P. V. Cherepanov, J. Choi, B. H. R. Suryanto, R. Y. Hodgetts, J. M. Bakker, F. M. Ferrero Vallana and A. N. Simonov, *Joule*, 2020, **4**, 1186–1205.
- 9 C. D. Dorich, R. T. Conant, F. Albanito, K. Butterbach-Bahl, P. Grace, C. Scheer, V. O. Snow, I. Vogeler and T. J. van der Weerden, *Curr. Opin. Environ. Sustain.*, 2020, **47**, 13–20.
- 10 K. Yamashita, Z. Liu, K. Iyoki, C. T. Chen, S. Miyagi, Y. Yanaba, Y. Yamauchi, T. Okubo and T. Wakiyara, *Chem. Commun.*, 2021, **57**, 1312–1315.
- 11 S. Yamaguchi, P. Hu, H. Ya, P. Xiao, A. Nakata, T. Miyazaki, Y. Morikawa, J. N. Kondo, K. Tange, K. Tonokura, M. Takemoto, Y. Yonezawa, T. Yokoi, K. Iyoki, T. Okubo and T. Wakiyara, *Microporous Mesoporous Mater.*, 2025, **388**, 113550.
- 12 M. Jablonska, *RSC Adv.*, 2022, **12**, 25240–25261.
- 13 S. Mohan, P. Dinesha and S. Kumar, *Chem. Eng. J.*, 2020, **384**, 123253–123262.
- 14 H. Li, X. Yi, J. Miao, Y. Chen, J. Chen and J. Wang, *Catalysts*, 2021, **11**, 906–920.
- 15 Y. Inomata, S. Hata, M. Mino, E. Kiyonaga, K. Morita, K. Hikino, K. Yoshida, H. Kubota, T. Toyao, K.-i. Shimizu, M. Haruta and T. Murayama, *ACS Catal.*, 2019, **9**, 9327–9331.
- 16 B. Suzumura, K. Tanaka, K. Kitazume, S. Hioki, A. Kubo and M. Iwamoto, *Catal. Sci. Technol.*, 2023, **13**, 4131.



- 17 K. Tanaka, B. Suzumura, K. Kitazume, H. Suzuki, H. Teduka and M. Iwamoto, *Catal. Lett.*, 2024, **154**, 2090.
- 18 J. Long, S. Chen, Y. Zhang, C. Guo, X. Fu, D. Deng and J. Xiao, *Angew. Chem., Int. Ed.*, 2020, **59**, 9711–9718.
- 19 A. G. Ramu, R. Renukadevi, P. Silambarasan, I-S. Moon, M. Govindarasu and D. Choi, *J. Environ. Chem. Eng.*, 2023, **11**, 110751.
- 20 D. Wang, Z. W. Chen, K. Gu, C. Chen, Y. Liu, X. Wei, C. V. Singh and S. Wang, *J. Am. Chem. Soc.*, 2023, **145**, 6899.
- 21 S. B. Rawal, S. Bera and W. I. Lee, *Catal. Lett.*, 2012, **142**, 1482–1488.
- 22 M. Grätzel, *Nature*, 2001, **414**, 338–344.
- 23 T. Suguro, F. Kishimoto, N. Kariya, T. Fukui, M. Nakabayashi, N. Shibata, T. Takata, K. Domen and K. Takanabe, *Nat. Commun.*, 2022, **13**, 5698.
- 24 T. Suguro, F. Kishimoto and K. Takanabe, *Energy Fuels*, 2022, **36**, 8978–8994.

